Bioresource Technology 161 (2014) 91–101

Contents lists available at ScienceDirect

Bioresource Technology

journal homepage: www.elsevier.com/locate/biortech

Hydrothermal carbonization (HTC): Near infrared spectroscopy and partial least-squares regression for determination of selective components in HTC solid and liquid products derived from maize silage

M. Toufiq Reza [a,*], Wolfgang Becker [b], Kerstin Sachsenheimer [b], Jan Mumme [a]

[a] APECS Group, Leibniz Institute for Agricultural Engineering (ATB), Max-Eyth-Allee 100, Potsdam 14469, Germany
[b] Energetische Systeme, Fraunhofer Institut für Chemische Technologie (Fh-ICT), Joseph-von-Fraunhoferstr. 7, Pfinztal 76327, Germany

HIGHLIGHTS

- HMF and furfural produced during HTC are degraded on HTC 250 after 180 min.
- NIR spectroscopy can be applied for both solid and liquid products of HTC.
- NIR accompanying with PLSR can be applied for quantitative prediction of HTC products.

ARTICLE INFO

Article history:
Received 24 January 2014
Received in revised form 1 March 2014
Accepted 3 March 2014
Available online 13 March 2014

Keywords:
Hydrothermal carbonization
HTC biochar
NIR spectroscopy
Principle component analysis
Partial least-squares regression

ABSTRACT

Near-infrared (NIR) spectroscopy was evaluated as a rapid method of predicting fiber components (hemicellulose, cellulose, lignin, and ash) and selective compounds of hydrochar and corresponding process liquor produced by hydrothermal carbonization (HTC) of maize silage. Several HTC reaction times and temperatures were applied and NIR spectra of both HTC solids and liquids were obtained and correlated with concentration determined from van-Soest fiber analysis, IC, and UHPLC. Partial least-squares regression was applied to calculate models for the prediction of selective substances. The model developed with the spectra had the best performance in 3–7 factors with a correlation coefficient, which varied between 0.9275–0.9880 and 0.9364–0.9957 for compounds in solid and liquid, respectively. Calculated root mean square errors of prediction (RMSEP) were 0.42–5.06 mg/kg. The preliminary results indicate that NIR, a widely applied technique, might be applied to determine chemical compounds in HTC solid and liquid.
© 2014 Elsevier Ltd. All rights reserved.

1. Introduction

The world is facing two large challenges in energy sector, e.g., renewable sources and their sustainability. According to the United Nations report, up to 77% of the world's energy in 2050 could come from renewable sources [UN report, 2007]. Lignocellulosic biomass like primary (straw, grasses) and secondary agricultural residues (rice hulls, corn cobs, straw-manure mixtures) have no conflicts with the food versus fuel issue. Moreover, biomass is the third largest source of energy after petroleum and coal. This is the only renewable energy source with carbon in the structure, compared to wind, solar, and water [IPCC, 2011]. However, the handling characteristics, lower bulk density, high ash content, and lower energy content hindered the usage of lignocellulosic biomass for energy production [IPCC, 2011]. An efficient method of producing renewable, sustainable energy from lignocellulosic biomass is beneficial to overcome the current crisis.

Hydrothermal carbonization (HTC) is one of the promising thermochemical processing of biomass for producing hydrochar and value-added chemicals. The history of HTC goes back to 1913, when Bergius made an attempt of producing synthetic coal from cellulose. However, the similar concept was rediscovered recently aiming to mitigate the emission of green-house gases, to improve energy, and food security, and to use the most abundant form of

Abbreviations: HTC, hydrothermal carbonization; NIR, near infrared spectroscopy; HHV, higher heating value; HMF, hydroxymethyl furfural; PLS, partial least squares; PLSR, partial least squares regression; OSC, orthogonal signal correction; JK, Jack Knifing; VN, vector normalization; KM, Kubelka–Munk; EMSC, extended multiplicative scatter correction; RMSEC, root mean square error of calibration; RMSECV, root mean square error of cross validation; SNV, standard normal variate; PCA, principal component analysis; PC, principal component; DI water, de-ionized water; PID controller, proportional-integral-differentiate controller.

* Corresponding author. Tel.: +49 (331) 5699 922; fax: +49 (331) 5699 849.
E-mail address: treza@atb-potsdam.de (M.T. Reza).

http://dx.doi.org/10.1016/j.biortech.2014.03.008
0960-8524/© 2014 Elsevier Ltd. All rights reserved.

carbon to value-added products. Recent studies mentioned that HTC is a promising technology for converting biomass into lignite-type coal [Parschetti et al., 2013], into liquid biofuel [Hoekman et al., 2011], into a soil amender [Libra et al., 2011; Rillig et al., 2010], into a carbon material for liquid contaminant adsorption [Regmi et al., 2012], into nanostructure carbon material [Cui et al., 2006], into a carbon catalyst [Hu et al., 2010; Yu et al., 2012], or into carbon material for increasing fuel cell efficiency [Titirici and Antonietti, 2010].

Subcritical water has the ionic product maximum in the temperature range of 200–280 °C [Bandura and Lvov, 2006]. When biomass is treated with subcritical water, organic components, e.g., lignin, cellulose, hemicelluloses degrade to some extent. During HTC, first hydrolysis of the extractives, hemicellulose, and cellulose followed by dehydration, and followed by decarboxylation, condensation, polymerization, and aromatization take place in the liquid phase [Funke and Ziegler, 2010; Reza et al., 2014]. Although the overall reaction chemistry follows mainly the stated reaction paths, each of the individual HTC reaction has their own reaction kinetics and probably catalyzed by one another [Reza et al., 2013b]. The HTC reactions in the liquid phase are mainly responsible for the production of so-called liquid biocrude [Kruse et al., 2013], which considers as the main precursor of solid hydrochar. Thus, the quality of hydrochar depends on the composition of process liquor and which makes the HTC process more unique compare to other thermochemical conversion processes [Libra et al., 2011]. Besides HTC reaction temperature and reaction time, the liquid phase reactions as well as the formation of the hydrochar also depend heavily on the feedstock [Wiedner et al., 2013]. HTC process liquor is often defined as the waste water and requires proper treatment prior to discharge into the environment, even after successive recycling [Uddin et al., 2013]. However, the high strength HTC process liquor can be an effective feedstock for biogas production via anaerobic digestion [Wirth and Mumme, 2013], which can potentially contribute to the overall economics besides treating waste water. So, the knowledge about the chemistry and kinetics of liquid phase as well as solid phase of specific feedstock are necessary for comprehensive HTC process and product optimization.

Optical spectrometry is a universal tool for characterization of solid and liquid products. The signature spectra can reveal the chemical information, which will reduce the extensive, tedious laboratory analyses. A successful optical technique is often necessary for designing in-line or on-line process control, thus helps to scale up processes from batch to continuous, and from small to large scale. For instance, NIR spectroscopy has proved to be a valid analytical tool for food products quality assurance [Blanco and Villarroya, 2002; Chen and He, 2007]. As a multivariate and rapid technique NIR spectroscopy offers the possibility to determine concentration of selective substances. The solid as well as the liquid phase can be measured with adjusted probes and measurement configurations. Several applications of the use of NIR spectroscopy to construct models for evaluating components content can be found in the literature. For example, it has been employed to analyze carotenoids content in maize [Brenna and Berardos, 2004], organic matters in soil [Fidencio et al., 2002], arachidonic acid in powdered oil [Yang et al., 2010], and α-tocopherol in vegetable oils [Szlyk et al., 2005]. However, by far the author's knowledge, NIR was conducted for neither hydrochar nor HTC process liquor yet.

The main goal of this work was to investigate the use of NIR for the detection of selected HTC products by means of Partial least-squares regression. Further objectives were to determine quantitatively the concentration of selective soluble organic products, to describe the physical and chemical changes of both hydrochar and process liquor with different HTC temperature and time, and correlate the chemical analyses with the NIR spectra.

2. Methods

2.1. Hydrothermal carbonization

Maize silage was acquired from a locally grown test site at Leibniz Institute for Agricultural Engineering (ATB), Potsdam, Germany. The feedstock's size was reduced to 5 ± 3 mm. Moisture content of the feedstock was 13 ± 1 wt%. Around 50 g of maize silage was weighed in a beaker, transferred into a 1 L Parr reactor stirred reactor (reactor series 4520, IL, USA). DI water of 600 ml was weighed by same balance (maintain 1:12 maize silage, water ratio) and poured into the reactor. The experimental condition was set either 200 or 250 °C for holding time 20, 60, 180, and 300 min with the 3 K min^{-1} heating rate. There was one additional experiment performed at 230 °C for 1 h. The reaction temperature was controlled by a Parr PID temperature controller (4520 series). The accuracy of the controller was set at ±1 K. The pressure was not controlled, rather monitored during the reaction. The content was stirred continuously during the hydrothermal treatment at 180 rpm. After the end of reaction period, the heater was turned off and let the reactor cooled down naturally. It took 3–4 h to cool down from 250 to 25 °C (about 20 min from 250 to 180 °C), while pressure drops from 4–4.5 to 0.2–0.5 MPa. The gaseous product was purged in the hood; the solid product was filtered using a folded filter paper (ROTH Type 113 P filter) for 20 min. The process liquid was stored into a 4 °C refrigerator for further analyses. The solid product was dried in a heating oven for overnight at 105 °C. Dried solid product was placed into a zip-lock bag and stored for further use. Each individual experiment was carried at least three times and the solid products and process liquors were mixed prior to further analyses for minimizing experimental errors.

2.2. Chemical analyses

A modified van-Soest method using the ANKOM A200 Filter Bag Technique (FBT) was used to determine the contents of hemicellulose, cellulose, lignin, and aqueous soluble compounds in solid samples [Reza et al., 2014]. The solid samples are first crushed and sieved to the desired particle size (20–65 mesh) and were dried at 105 °C for 24 h prior to the analysis. The contents of hemicellulose, cellulose, and lignin were calculated from the difference of neutral detergent fiber (NDF), acid detergent fiber (ADF), acid detergent liquid (ADL), and ash as shown following;

$$\text{Extractives}\ (\%) = 100 - \text{NDF}\ (\%)$$
$$\text{Hemicellulose}\ (\%) = \text{NDF}\ (\%) - \text{ADF}\ (\%)$$
$$\text{Cellulose}\ (\%) = \text{ADF}\ (\%) - \text{ADL}\ (\%)$$
$$\text{Pseudo-lignin}\ (\%) = \text{ADL}\ (\%) - \text{Ash}\ (\%)$$

According to modified van-Soest method, biomass and hydrochar are divided into five components only in this method and any change of one component will affect the others. The method is based on extraction of fibrous substances using NDL, ADF, and ADL. The method is well-established for raw biomass, however, several scientists were adopted this technology for hydrochar analysis as well [Parschetti et al., 2013; Reza et al., 2013b, 2014; Uddin et al., 2013]. The solid residue left after ADL is pseudo-lignin and ash. Ash, determined separately by muffle furnace according to ASTM D2974, subtracted from lignin and ash weight from fiber analysis, to find lignin content. So, pseudo-lignin is not measured directly and this is one of the main shortcomings of this method. The higher heating value (HHV) was calculated using the correlation of Boie and presented as dry-ash-free basis (Boie, 1953).

Liquid phase pH was measured directly after filtration using a WTW inoLab pH/Cond 720 with a Sen Tix probe. Solid pH was measured after drying the solid residue and then mixing with water in

a 1:10 w/w (solid:water) ratio. The sample-water mixture was shaken for 15 min before the pH was measured.

The concentrations of selective volatile organic compounds (5-HMF, 2-furfural, phenol, catechol, cresol, and resorcinol) in process liquid were measured using a modified ICS 3000 Dionex (Thermo Scientific) with a UV detector (wavelength 280 nm) and Knaur Eurosphere II (C 18) column. A 15% acetonitrile (85% DI water) was used as mobile phase in the IC. Column temperature was set at 23 °C and flow rate was 1.0 ml min^{-1}. Sugars (glucose, sucrose, fructose, xylose) and organic acids (acetic, formic, lactic acid) concentration in the HTC process liquor were measured by Thermo Scientific Dionex Ultimate 3000 UHPLC equipped with Eurokat H (300 × 8 mm) column, RI-71 (refractive index) detector, and Ultimate 3000 autosampler. Sulfuric acid of 0.01 N was used as mobile phase in the UHPLC. The flow rate was maintained at 0.8 ml min^{-1} and pressure 80 bar. The oven temperature for UHPLC was set at 35 °C during the analyses of sugars and acids in the liquid solution.

Total organic carbon (TOC) in the process liquors was measured by a TOC Analyzer 5050 A (Shimadzu Scientific Instruments, Columbia, MD, USA). The precision of TOC analysis was <2%.

2.3. NIR instrumentation and data collection

Near infrared spectral measurements were done with a Carl Zeiss diode array spectrometer system in the spectral range from 900 to 2200 nm with a spectral resolution of about 6 nm wavelength. Each spectrum was measured with 20 accumulations and an integration time of 100 ms. All the hydrochar and corresponding process liquor samples were investigated individually. Each sample was measured at least three times for better precision in reflection with NIRS. The liquid samples were filled in a petri dish with a filling level of 2 mm and measured in reflection with an OMK 500 fiber coupled probe (Carl Zeiss). The distance between sample surface and probe was 2 cm. Hydrochar samples were measured in the same way whereby the petri dishes were completely filled.

2.4. NIR data processing and development of the calibration model

In addition to the valuable sample information, the NIR spectra comprise chemical information i.e., substance specific absorption bands and physical influences like light scattering or noise. Hence it is necessary to pre-treat spectral data before modeling, to extract only relevant information to obtain reliable, accurate, and stable prediction models. At present, there are many pre-processing methods, such as smoothing, derivative, extended multiplicative scatter correction (EMSC), orthogonal signal correction (OSC), Jack Knifing (JK), vector normalization (VN), Kubelka–Munk (KM). The details of these pretreatment methods can be found elsewhere [Luypaert et al., 2004; Yang et al., 2010]. The data pre-treatment methods are intended first to reduce noise, light scattering and temperature effects to the spectra, and then to improve spectral resolution through. In this study, six data pre-processing methods were applied accordingly, namely OSC and EMSC for liquor and JK, VN, OSC, and KM for solid analysis.

NIR spectra were analyzed with principal component analysis (PCA) and concentrations of different substances in the samples were correlated with NIR spectra with partial least square regression (PLSR). For the analysis and evaluation of the spectra the software Unscrambler® from CAMO was used. The data set was split randomly into a training ($n = 75$) and a validation set ($n = 25$). The optimum number of PLS factors in the calibration models was determined by cross-validation and by the RMSEC(V). Overfitting of the models was avoided by controlling the explained variance of the prediction models [Fearn et al., 2002]. The relative performance of the established model was assessed by the required number of factors, by the root mean square error of calibration (RMSEC), and the root mean square error of cross-validation (RMSECV). The complete spectrum was used for model generation or specific spectral regions were selected with the Jack-Knifing procedure to improve model performance.

3. Results and discussion

3.1. Physico-chemical properties of hydrochar

Table 1 shows the mass yield (ratio of dry hydrochar and dry biomass weight) along with solid pH, fiber analysis, HHV, and few volatile organic components. From Table 1, it can be found that hemicellulose degrades more than 90% in the first 20 min even at the lowest HTC temperature. Cellulose concentration in the HTC biochar increases about 41%, after 20 min at HTC 200, which might be the reflection of hemicellulose degradation. However, the concentration of cellulose decrease with the increase of holding time and after 6 h of reaction time at 200 °C, overall cellulose concentration decreased of 23%. Although pure cellulose does not degrade before 220 °C in hydrothermal media [Diakité et al., 2013], cellulose in biomass often degrade to some extent as low as 200 °C [Reza et al., 2013b]. Hydrolysis products from hemicellulose and other extractives might catalyze the cellulose degradation at lower HTC temperature. At 250 °C, more than 78% cellulose of maize silage was degraded in 1 h according to Table 1. (Pseudo)Lignin concentration increased at the increase of severity of HTC throughout this study. At 200 °C after 6 h of reaction, the (pseudo-)lignin concentration was 38.3%, which was more than 5 times of the lignin originating in the raw biomass. If we assume that lignin is inert and even then considering 45.4% mass yield, the theoretical lignin concentration could be 15.4% at HTC 200, 6 h biochar, which means

Table 1
Physico-chemical analyses of hydrochar derived from maize silage. HHV, higher heating value; db, dry basis; HMF, hydroxymethyl furfural.

Condition	Time (min)	Mass yield (%)	pH	Extractives (%)	Hemicellulose V(%)	Cellulose[1] (%)	(Pseudo-) Lignin (%)	Ash (%)	HHV (MJ/kg db)	HMF (mg/kg db)	Furfural (mg/kg db)	Phenol (mg/kg db)
Raw	–	–	4.8	27.3	26.3	32.7	7.0	6.7	15.6	–	–	–
HTC 200	20	51.8	4.4	36.9	2.7	46.4	9.5	4.5	21.6	2.1	16.2	3.9
HTC 200	60	49.2	4.8	29.2	3.2	38.7	25.1	3.9	23.0	3.8	7.1	8.4
HTC 200	180	47.4	4.3	38.9	1.7	29.7	27.2	2.6	24.9	5.7	8.9	23.9
HTC 200	360	45.4	4.1	31.5	2.1	25.3	38.3	2.8	25.6	3.5	7.4	25.8
HTC 250	20	41.0	5.4	37.6	6.1	22.0	32.4	1.9	22.4	1.1	3.7	14.6
HTC 250	60	39.4	6.0	45.2	1.1	7.4	44.4	1.9	27.8	0.3	2.6	16.6
HTC 250	180	39.3	5.9	43.2	0.4	4.6	49.2	2.6	28.4	0.0	2.4	27.0
HTC 250	360	39.6	6.0	34.9	0.3	4.3	58.3	2.3	30.3	0.0	1.9	29.7
HTC 230	60	45.3	4.7	40.1	4.8	25.2	24.6	4.7	22.3	3.1	8.1	27.4

[1] Cellulose amount is calculated by van-Soest fiber analysis.

there might be the production of lignin-like substances (pseudo-lignin) during HTC. According to the literatures, hydrochar is difficult to distinguish from lignin by van-Soest fiber analysis [Sevilla and Fuertes, 2009; Reza et al. 2014]. Moreover, some reaction intermediates might react with the existing lignin and attached with the lignin. As a result, the residues left after ADL treatment of hydrochar can be compared as lignin and here we named it as pseudo-lignin. As the (pseudo-)lignin percentage increases with the increase of HTC time and temperature, HHV of the HTC biochar increases as well. In fact, HHV of HTC 200, 6 h biochar was 64% and HTC 250, 6 h biochar was 94% more than HHV of raw maize silage. Raw maize silage had relatively higher ash content of 6.7%, probably due to the presence of loose dirt. However, with the increase of HTC temperature and time, the ash content was decreased up to 1.9% (HTC 250, 1 h). Holding HTC temperature at 250 °C more than 1 h yielded a small increase of ash, compared to HTC 250, 1 h, which might be resulted from the decrease of overall mass yield. However, the increase was small enough to draw any certain conclusion, as the experimental error for ash analysis is around ±0.5%. From Table 1, the presence of several volatile organic compounds (VOC) like HMF, furfural, phenol can also be observed. The presence of several VOCs often makes the hydrochar toxic, and hydrochar with higher VOC is prohibited for soil usage [Libra et al., 2011; Becker et al., 2013]. There might be a possibility of entrapping such VOCs in the hydrochar pores or simply adhere in the hydrochar surface. It has been well studied that with the increase of HTC temperature and time, the hydrochar becomes more porous than raw feedstock [Diakité et al., 2013; Libra et al., 2011]. However, with the increase of reaction temperature and holding time, the VOCs concentration decreases as they are possibly degraded into smaller substances like acids or alcohols [Funke and Ziegler, 2010; Reza et al., 2014; Sevilla and Fuertes, 2009]. In fact, at 250 °C, 1 h there was no detectable HMF found in the biochar. Meanwhile, the concentration of phenol in the hydrochar was increasing with HTC reaction time for both temperatures. In fact, the higher HTC temperature and higher reaction time yields the maximum phenol in hydrochar in this study. Increase of phenol in the solid phase with process severity is in agreement with the findings reported by Becker et al. (2013). It can also be found from the literature that raw lignocellulosic residues have some phenol, which can be concentrated in the hydrochar produced from 190 to 250 °C [Becker et al., 2013]. After 270 °C, phenol concentration in the hydrochar increases very rapidly due to lignin degradation [Sevilla and Fuertes, 2009], which is of the reason in this study not to perform HTC above 250 °C.

3.2. Chemical analyses of HTC process liquor

Table 2 presents the chemical analyses of HTC process liquor, where maize silage was treated at various HTC conditions. TOC was the highest in the short reaction time for 20 min at HTC 200, which was 28% more than the TOC produced by 20 min at HTC 250. In HTC 200 liquid the concentration of HMF accumulate until 1 h and then degrade drastically. In fact, at HTC 250, after 3 h, no HMF was found in the HTC process liquid. Similar to HMF, furfural is also found unstable under higher HTC temperature, as the highest concentration observed at HTC 200 after 20 min and no furfural was found in the HTC 250, 3–6 h process liquid. This might indicate that, furfural degradation favors higher HTC temperature as well. Phenol concentration was lower than HMF or furfural, yet can be found in HTC 200 process liquid throughout the reaction time until 6 h. Meanwhile, relatively more phenol was found in HTC 250 process liquid, which is consistent with hydrochar analysis.

Sugars molecules like glucose, fructose, xylose, and sucrose are hydrolysis products of starch, hemicellulose, and cellulose [Hoekman et al., 2011]. In subcritical water, the sugar molecules are very tentative to degrade into smaller acids like formic acid, acetic acid, or lactic acid; can also undergo for further dehydration reaction and produce HMF, furfural, anhydroglucose, erythrose, etc.; or even directly degrade into water and CO_2 [Parajo et al., 1993; Sevilla and Fuertes, 2011]. As a result, the maximum concentrations of sugars were observed at the lower reaction time and temperature. However, the degree of degradation was different for each sugar as glucose degradation was found slower that xylose or sucrose. As a result, a moderate concentration of glucose was observed until 60 min at HTC 200. Again, 250 °C was found high enough to degrade almost all glucose in less than 20 min. Unlike sugars, concentrations of organic acids such as acetic acid, formic acid, and lactic acid, which are possible products of degradation of simple sugars and/or the reactive furfural derivatives, found lower when the sugar concentration was high. Lactic acid was the exception of this case, as the lactic acid usually present in the raw dry maize silage [Wirth and Mumme, 2013], again can be a by-product of direct hydrolysis of extractives in the lignocellulosic biomass [Sevilla and Fuertes, 2009]. Formic and acetic acid concentrations were increased with the increase of reaction time for HTC 200, whereas at 250 °C their concentrations were decreased with the reaction time longer than 180 min.

3.3. NIR spectra of hydrochar and HTC process liquor

Fig. 1 shows the reflection spectra of the solid hydrochar (Fig. 1a) and the HTC process liquor samples (Fig. 1b). In the NIR study, a HTC 230, 1 h sample was added to the set of the different HTC 200 and HTC 250 samples. The main intention was to check the consistency of the NIR experiments. HTC 200 samples showed more peaks than HTC 230 and HTC 250, and the peaks wore more prominent at lower reaction times. The peak around 1350–1450 nm, possibly corresponds to CH, OH, or NH [Weyer, 1985], can be observed only in HTC 200 samples. Again, a small peak appeared around 1650–1750 nm, possibly corresponds to CH, was only found for HTC 200. The largest peak around 1820–1950 nm,

Table 2
Chemical analyses of HTC process liquor using GC and HPLC. TOC, total organic content, HMF, hydroxymethyl furfural.

Condition	Time (min)	Glucose (mg/l)	Xylose (mg/l)	Sucrose (mg/l)	Lactic acid (mg/l)	Formic acid (mg/l)	Acetic acid (mg/l)	HMF (mg/l)	Furfural (mg/l)	Phenol (mg/l)	TOC (mg/l)
HTC 200	20	3330.0	2010.0	3180.0	4620.0	335.0	1340.0	1335	1382	23	17777
	60	2767.0	0.0	587.0	6468.0	4240.0	1787.0	4343	1302	45	15205
	180	150.0	80.0	425.0	6116.0	5062.0	1500.0	2120	646	48	10111
	360	152.0	0.0	421.0	4985.0	4871.0	1923.0	917	285	67	9468
HTC 250	20	85.0	101.0	407.0	5578.0	1918.0	1998.0	1707	698	108	11553
	60	112.0	0.0	372.0	4999.0	3616.0	2122.0	571	203	139	9241
	180	0.0	0.0	458.0	4863.0	2728.0	300.0	0	8	109	9094
	360	0.0	0.0	416.0	4296.0	2611.0	500.0	0	12	91	7980
HTC 230	60	227.0	127.0	691.0	9133.0	600.0	3852.0	2419	775	172	16842

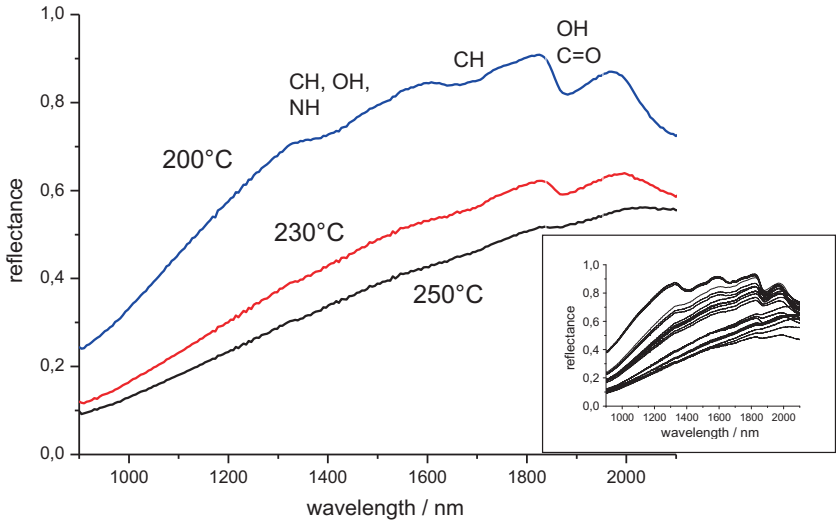

Fig. 1a. Reflectance spectra of solid samples produced at different process temperatures. The process time was 60 min for all samples. Main absorption bands which can be assigned to main functional groups are indicated. Absorption bands decrease with increasing process temperature.

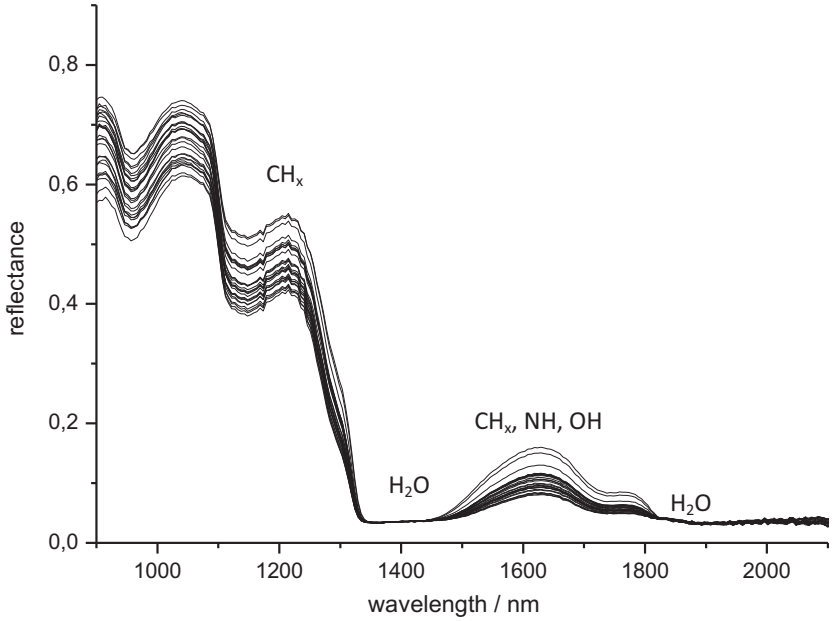

Fig. 1b. Reflection spectra from the HTC liquids. Total absorption of light by water is indicated. CH_x indicates the presence of either CH, CH_2 or CH_3.

corresponding to OH and C=O [Weyer, 1985], appeared for all samples. However, the reflectance of the later peak seemed to decrease with higher HTC temperature and longer time. It is obvious from the NIR spectra that the hydrochar compositions are different for different HTC condition, although the starting feedstock was same maize silage.

In the NIR spectra of all HTC process liquors, a very low reflectance was found around 1350–1450 nm and above 1820, due to IR absorbed by water [Yang et al., 2010]. Water is a very effective for absorption of light, in the NIR spectral range with penetration depths of only 1 mm to about 1.5 mm. The rest of the NIR wavelength range was dominated by CH_x (CH, CH_2, or CH_3), NH and OH absorption. Bands around 1450–1800 nm are known to show good correlation causing variation in the measured reflection spectra in dependence of the amount of contained substances [Szlyk et al., 2005]. Besides that several early reflectance prior to 1200 nm corresponding for CH_x were observed for every liquor samples. This might be attributed to small suspended particles causing scattering of the incoming light (IR). As the measured spectra consist of absorption and diffuse reflection, and the correlation between the two effects, this must be considered in the evaluation and treatment of the spectra. From the liquor NIR spectra, it can be found that there are many common compounds in the process liquor. Prediction of the various chemical compositions in both hydrochar and process liquor from NIR spectra will be discussed in the following sections.

3.4. Principal component analysis (PCA) of NIR spectra

Fig. 2 shows the result of the PC1–PC2 score plot of the solid hydrochar spectra (Fig. 2a) and the HTC process liquor spectra (Fig. 2b). In both cases, the NIR spectra were pretreated with standard normal variate (SNV) transformations and converted into Kubelka–Munk (KM) units. The two principal components (PC) for the spectral variances of solid hydrochars and HTC process liquors contain about 99% and 95% of the spectral information,

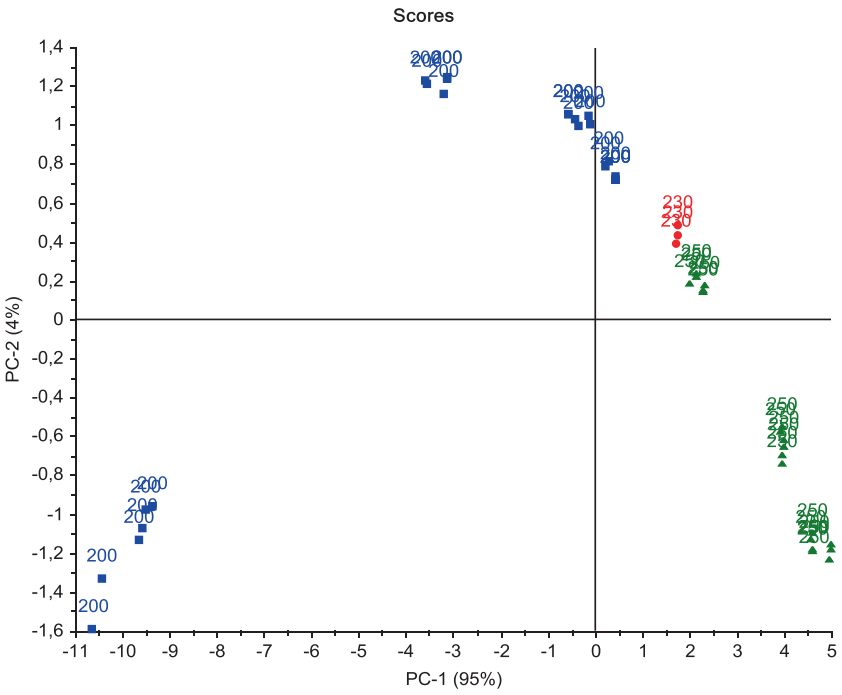

Fig. 2a. PCA of the spectra of solid HTC samples. Score plot of PC1 and PC2. The spectra were pretreated with standard normal variate (SNV). 99% of the spectral variation is explained by PC1 and PC2.

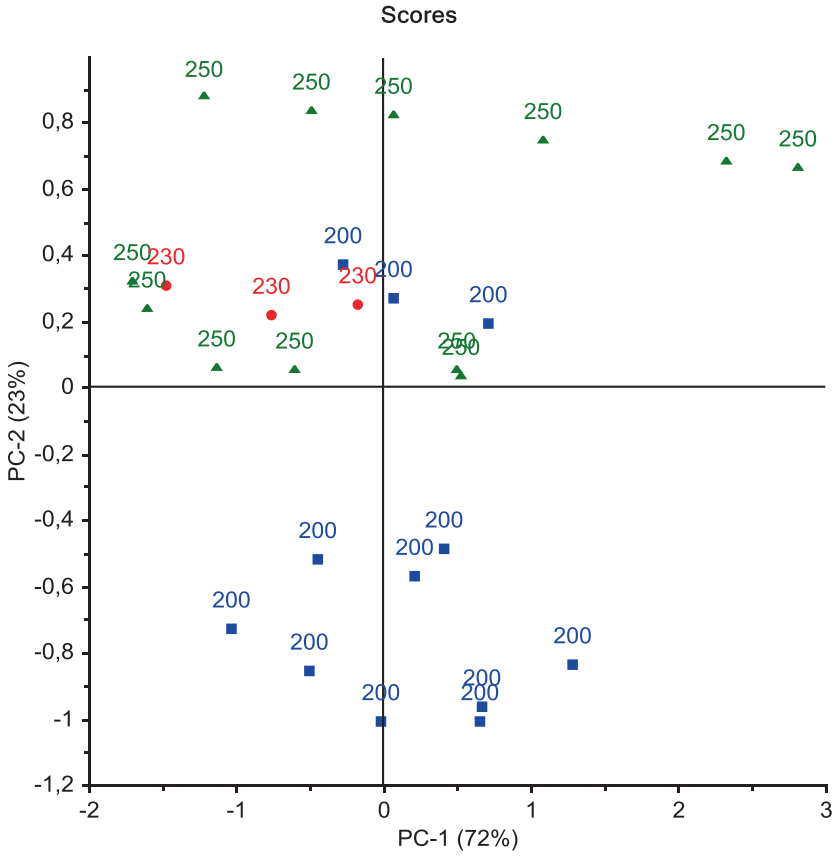

Fig. 2b. PCA of the spectra of liquid HTC samples. Score plot of PC1 and PC2. The spectra were pretreated with standard normal variate (SNV) transformation and converted into Kubelka–Munk units.

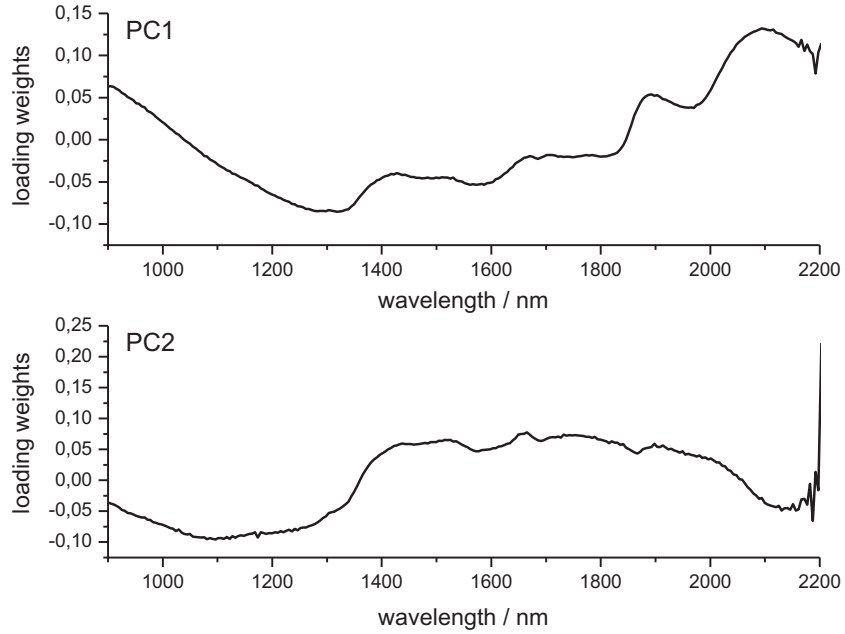

Fig. 3a. Loading weights of the PC1 and PC2 of the PCA in Fig. 2a.

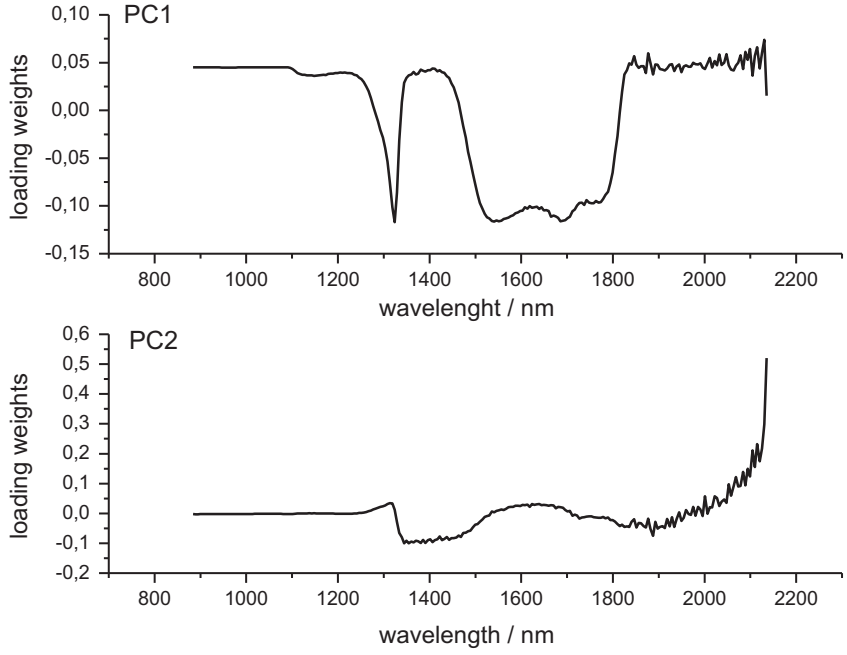

Fig. 3b. Loading weights of the PC1 and PC2 of the PCA in Fig. 2b. PC2 is relevant for the separation of the sample spectra according to process temperature.

respectively. Each score plot has several independent clusters, representing a dominance of certain compounds in these samples and consequently there are systematic information which can be exploited. For the solid hydrochar (Fig. 2a), two clusters from HTC 250 and HTC 230 were found very close, which might imply the sharing of similar components. In the score plot for process liquor, three well separated clusters can be found. Two clusters consist of the sample spectra with a process temperature of only 250 and 200 °C, respectively. The third cluster comprises samples of both process temperatures with 230 °C. It seems that this cluster represents a transition between other two clusters. The assignment of the process time to the scores revealed no clear cluster separation and is therefore not shown. The process time, however, must still be considered as a possible factor that causes spectral variations and thereby influences further evaluations.

The wavelength-depended loading weights of PC1 and PC2 are shown in Fig. 3 (Fig. 3a for solid and Fig. 3b for liquor). High values indicate the importance of the wavelength range and hence clustering. The main difference between the clusters was along PC1 for solid score plot and PC2 for liquor score plot. PC1 shows higher importance for the solids than PC2, whereas PC2 seems to have superior relevance for the HTC liquors. The PC1 loading for the liquor (Fig. 3b) represents the influencing factors like light scattering caused by dissolved particles or temperature shifts in the liquid, hence not directly correlated with chemical information. The main result of the PCA analysis indicates that there is systematic

Table 3
Result of PLSR prediction models for different chemical compounds from HTC process for liquid fraction. Each sample was measured three times.

Chemical compound	Num. factors	Num. spectra	Pre-treatment spectra	Corr. coeff. calibr.	Corr. coeff. valid.	Conc. range compound [mg/l]	RMSEC [mg/l]	RMSECV [mg/l]
HMF	6	9	OSC	0.9715	0.7509	0–4343	217	868
Formic acids	7	9	EMSC	0.9886	0.7345	335–5062	245	1105
Glucose	7	9	EMSC	0.9957	0.8914	0–3333	115	562
Xylose	6	9	EMSC	0.9809	0.6857	0–140	9.9	37.5
Acidic acid	5	9	EMSC	0.9364	0.7172	0–3852	245	1066
Lactic acid	5	9	EMSC	0.9662	0.7979	4296–9133	358	847
Furfural	5	9	EMSC	0.9683	0.8669	7–140	121	242
Phenol	4	9	EMSC	0.9805	0.9407	20–180	4.3	13.6
Ash	6	9	EMSC	0.9738	0.7833	0.9–3	0.14	0.39

OSC, orthogonal signal correction; EMSC, extended multiplicative scatter correction.
RMSEC, root mean square error of calibration.
RMSECV, root mean square error of cross validation.

information in the spectra, which can be used for correlation of contained substances produced by the HTC process.

3.5. Correlation of NIR spectra with chemical analysis data

All NIR spectral data were statistically validated for predicting various chemical compounds in the hydrochar and HTC process liquor samples. During the calibration development, several spectral outliers were detected. The outlier eliminations were an essential step in the optimization procedure of the model development. As described earlier NIR spectra provides valuable information regarding the organic structural changes for both hydrochar and HTC process liquor. PCA analysis confirms the agreement and indicates that PLS might be useful for correlation of chemometric methods with NIR spectra.

PLS models were developed using eighteen samples (nine for hydrochar and other nine for process liquor) based on the selected 27 NIR spectra (including 3 repetitions) of the hydrochar and HTC process liquor samples, respectively. The prediction capability was evaluated by correlation coefficient (r), RMSEC and RMSECV. It was expected to have ideal models, when they show low RMSEC and RMSECV as well as a high correlation coefficient (r). The optimum number of PLS-factors were selected by the explained variance and RMSEC(V), whereby the aim is to use as few number of PLS-factors as possible. The model stability will be improved and at the same time a low REMSEC(V) value with adopting lower acceptable PLS-factors. An increase in the RMSEC(V) indicates that the data have been overfitted by incorporating spectral information into the model that is not related to the specific compounds. That is why the optimum number of PLS-actors varies between 3 and 7 for different chemical compounds in either solid or liquid samples.

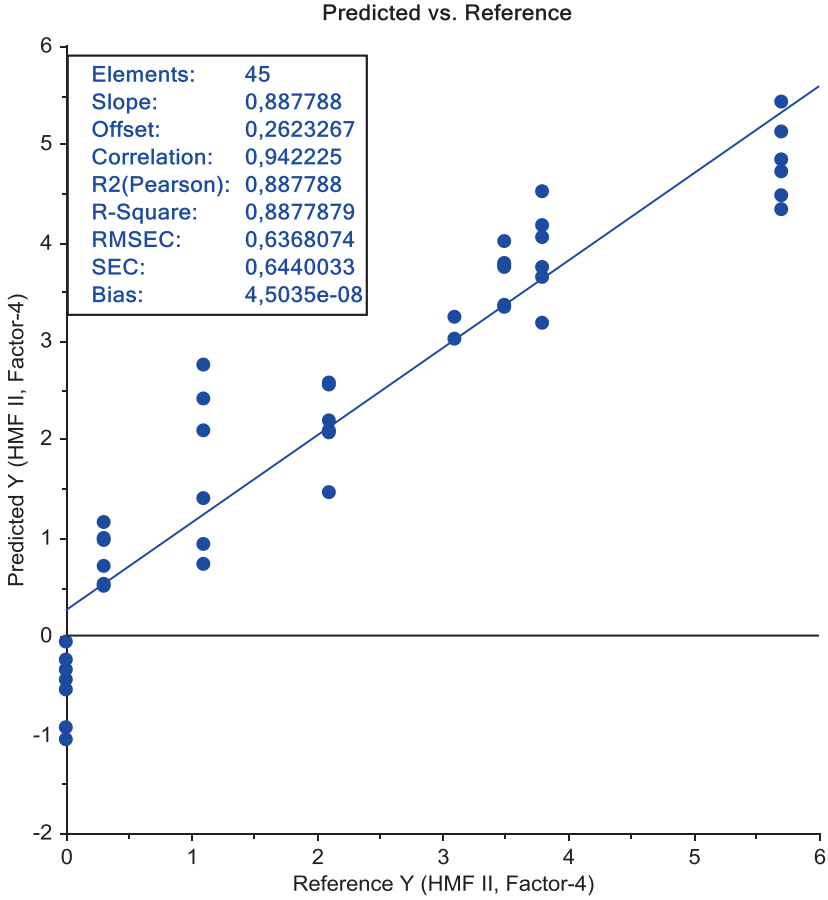

Fig. 4a. Result of the PLS regression of HMF chemical with the NIR spectra of the solid fraction. The model consists of 4 factors. Spectral range was reduced by Jack-Knifing.

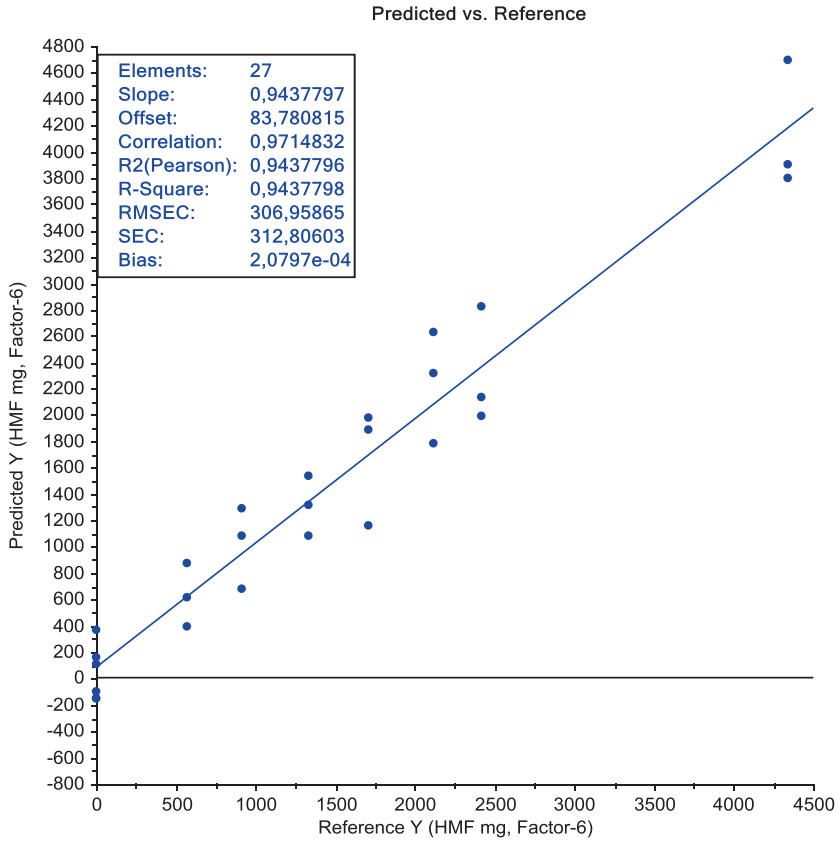

Fig. 4b. Result of the PLS regression of HMF chemical with the NIR spectra of the liquid fraction. The model consists of 6 factors. There were no outliers and spectra were pretreated with extended multiplicative scatter correction (EMSC).

The NIR spectra (Fig. 1) of the liquid fraction were correlated with several chemical components. All samples regardless of process temperature and process duration were used for the PLS modeling. The results of different spectral pretreatment models for the liquid samples are shown in Table 3. There were 9 liquor samples measured three times each. Partial least square regression (PLSR) was used for generating prediction models for determining the chemical components by spectral measurements similarly as shown in Fig. 4 for HMF in hydrochar (Fig. 4a) and in HTC process liquor (Fig. 4b) as an example. The concentration range for each chemical substance is given in column 7 of Table 3, as reliability of regression models is valid for the indicated range and should not be extended over these limits [Fearn et al., 2002]. The models developed with various pretreatments such as derivative, smoothing, SNV, EMSC and the combination of these pre-treatments were chosen to lower the number of factors and the RMSEC(V) values to improve model stability and prediction quality. The spectral pre-treatments shown in Table 3 are those where the lowest number of factors, RMSEC and RMSEC(V) were achieved. Prediction models for one varying substance would consist of only one factor in the ideal case. The higher number of factors in the present models for the liquid samples indicates that beside the abundance of substances in the liquid also varying factors like different sample processing temperature and time causes additional influencies hence must be modeled and number of PLS factors will increase. Number of factors (column 2 in Table 3) are varying from 4 (for phenol) to 7 factors (for HMF or glucose) in the prediction models.

As described above, spectral variations were caused by the different process temperatures and times, and also suspended particles in the liquid are scattering light. The scattering has a decisive influence to the quality and reproducibility of the spectral measurements and their effect must be either reduced by data pretreatment or by reducing their amount in the liquid, e.g., filtering, or emulsifying. Therefore, the liquids were shaken before every

Table 4
Results of PLSR prediction models for different chemical compounds from HTC process for solid fraction. Each sample was measured five times.

Chemical compound	Num. factors	Num. samples	Pre-treatment spectra	Corr. coeff. calibr.	Corr. coeff. valid.	Conc. range compound [mg/kg]	RMSEC [mg/kg]	RMSECV [mg/kg]
HMF	4	5	JK	0.9373	0.9162	0–5.7	0.66	0.76
Phenol	3	5	VN, OSC, JK	0.9395	0.9173	3.9–45.8	4.35	5.06
Furfural	3	5	OSC, JK	0.9880	0.9847	1.9–16.2	0.68	0.76
Ash	4	5	JK	0.9275	0.8983	1.9–4.7	0.36	0.42
Lignin	5	5	Raw	0.9797	0.9641	9.5–58.3	2.67	3.53
Cellulose	3	5	Raw	0.9781	0.9740	4.6–46.4	2.92	3.18
Hemicell.	6	5	KM	0.9672	0.9023	0.3–6.1	0.45	0.77

JK, Jack Knifing; OSC, orthogonal signal correction; VN, vector normalization; KM, Kubelka–Munk.
RMSEC, root mean square error of calibration.
RMSECV, root mean square error of cross validation.

measurement to ensure that there is no sedimentary deposition of the particles that could possibly falsify the spectra. With this, the coefficient of HMF was achieved 0.9715 and coefficient of determination r^2 was 0.9438 with 7 PLS factors and OSC pretreatment. RMSEC and RMSECV were 217 and 868 mg/l, respectively. Similar to HMF, other chemical constituents in the liquid were correlated with the NIR spectra and the results are presented in Table 3. EMSC is another pretreatment method, which can reduce the effect of light scattering to the spectra [Fearn et al., 2002; Martens and Naed, 1989]. Thus, the best prediction models i.e., lowest number of factors and lowest value of RMSEC and RMSECV for the liquid samples were achieved by EMSC spectral pre-treatment.

Correlation coefficients of calibration (CCC) in column 5 of Table 3 for liquid samples are found in the range from 0.9364 to 0.9957 and correlation coefficients of validation (CCV) in the range from 0.6857 to 0.9407. Validation method was used in the study was a full cross validation, where every sample is analyzed, model is generated, prediction is performed and correlated with the other samples and finally, CCV value is achieved. Therefore significant difference between the two values indicates that the prediction model stability must be improved by a higher number of samples or reducing variation in sample preparation, e.g., constant processing temperature. The correlations for various solid-phase components were found in the range of 0.9275–0.9880 for CCC and 0.8983–0.9847 for CCV values (Table 4). For instance the CCC for ash was the lowest 0.9275 with JK pretreatment validated for the range of 1.9–4.7 mg/kg and RMSEC and RMSECV were 0.36 and 0.42 mg/kg, respectively. Ash is very heterogeneous and can consist of various inorganic components, so prediction of ash from NIR spectra can be troublesome. On the other hand, furfural showed a CCV of 0.9880 with only 5 factors achieved with OSC and JK pretreatment, and RMSEC and RMSECV were 0.68 and 0.76 mg/kg, respectively. HMF showed a CCC of 0.9373 and coefficient of determination r^2 was 0.8878, as RMSEC and RMSECV were 0.66 and 0.76 mg/kg, respectively (Fig. 4a and Table 4). The suggested HTC process liquor models show a slightly higher number of PLS factors (4–7) (Table 3) compared to the solids models (3–6) (Table 4).The lower number of factors and higher correlations indicate that the variation in the solid samples are lower hence prediction models are more stable.

Precision of the prediction models for liquid and solid seems low (Figs. 4a and b). As agriculture feedstock consists of various components with various scattering potential, the regression models are still different from the prediction values. Correlation coefficients indicate that there is a significant correlation between the NIR spectral measurements and the chemical components. However, to improve the performance of the models a higher number of samples and standardization of measurement routines should be employed.

NIRS, as a nondestructive method could greatly simplify the analysis of individual compounds compared to the other physical and chemical methods, because no extraction step with organic solvents is required and samples can be readily analyzed in minutes. NIRS also offers the possibility to measure in-line and to control HTC process. Hence process and product optimization is feasible with NIRS monitoring method. Further selection of valuable information of spectral data and an explanation of the result could be needed to improve the model generalization and stability.

4. Conclusions

Hydrochar composition as well as chemical components in HTC process liquor varies with HTC temperature and time. This study has provided first results on a potential rapid determination method by NIR spectroscopy. The results indicate that determination of selective components (lignin, cellulose, hemicellulose, ash, HMF, furfural, phenol, sugars and organic acids) in both solid and liquid phases of HTC could be successfully performed through NIR spectroscopy combined with PLS models. However, as the models' number of factors and accuracies show high variations, further work are needed including the impact of different feedstock.

Acknowledgements

This research is supported by funds from the Bioenergy 2021 program delegated from the German Federal Ministry of Research and Education to Project Management Juelich (PtJ). Additionally, the authors would like to thank Ulf Lüder and Maja Werner for experimental support and Christoph Prautsch and Laureen Herkoltz for their support in analytical tasks.

References

Bandura, A., Lvov, A., 2006. The ionization constant of water over wide range of temperature and density. J. Phys. Chem. 35 (1), 793–800 (reference data).
Becker, R., Dorgerloch, U., Helmis, M., Mumme, J., Diakité, M., Nehls, I., 2013. Hydrothermally carbonized plant material: patterns of volatile organic compounds detected by gas chromatography. Bioresour. Technol. 130, 621–628.
Blanco, M., Villarroya, I., 2002. NIR spectroscopy: a rapid response analytical tool. Trends Anal. Chem. 21, 240–250.
Boie, W., 1953. Fuel technology calculations. Energietechnik 3, 309–316.
Brenna, O.V., Berardos, N., 2004. Application of near-infrared reflectance spectroscopy (NIRS) to the evaluation of carotenoids content in maize. J. Agric. Food Chem. 52, 5577–5582.
Chen, H., He, Y., 2007. Theory and application of near infrared reflectance spectroscopy in determination of food quality. Trends Food Sci. Technol. 18, 72–83.
Cui, X., Antonietti, M., Yo, S.H., 2006. Structural Effects If Iron Oxide Nanoparticles and Iron Ions on the Hydrothermal Carbonization of Starch and Rice Carbohydrates, vol. 6. Wiley-VCH Verlag GmbH & CO. KGaA, pp. 756–759.
Diakité, M., Paul, A., Jäger, C., Pielert, J., Mumme, J., 2013. Chemical and morphological changes in hydrochars derived from microcrystalline cellulose and investigated by chromatographic, spectroscopic and adsorption techniques. Bioresour. Technol. 150, 98–105.
Fearn, T., Naes, T., Isaksson, T., Davies, T., 2002. A User-friendly Guide to Multivariate Calibration and Classification. NIR publications, Chichester, UK.
Fidencio, P.H., Poppi, R.J., Andrade, C.D., Cantarella, H., 2002. Determination of organic matter in soil using near-infrared spectroscopy and partial least squares regression. Commun. Soil Sci. Plant Anal. 33 (9–10), 1607–1615.
Funke, A., Ziegler, F., 2010. Hydrothermal carbonization of biomass: a summary and discussion of chemical mechanisms for process engineering. Biofuels Bioprod. Biorefin. 4, 160–177.
Hoekman, S., Broch, A., Robbins, C., 2011. Hydrothermal Carbonization (HTC) of Lignocellulosic Biomass. Energy Fuels 25, 1802–1810.
Hu, B., Wang, K., Wu, L., Yu, S.H., Antonietti, M., Titirici, M.M., 2010. Engineering carbon materials from the hydrothermal carbonization process of biomass. Adv. Mater. 22 (7), 813–828.
IPCC, 2011. Special report on renewable energy sources and climate change mitigation. In: Summary for Policymakers. Cambridge University Press, Cambridge, United Kingdom.
Kruse, A., Funke, A., Titirici, M.M., 2013. Hydrothermal conversion of biomass to fuels and energetic materials. Curr. Opin. Chem. Biol. 17, 515–521.
Libra, J.A., Ro, K.S., Kammann, A., Funke, A., Berge, N.D., Neubauer, Y., et al., 2011. Hydrothermal carbonization of biomass residuals: a comparative review of the chemistry, process, and applications of wet and dry pyrolysis. Biofuels Bioprod. Biorefin. 2 (1), 89–124.
Luypaert, J., Heuerding, S., Heyden, Y.V., Massart, D.L., 2004. The effect of preprocessing methods in reducing interfering variability from near-infrared measurements of creams. J. Pharm. Biomed. 36, 495–503.
Martens, H., Naed, T., 1989. Mulivariate Calibration. JohnWiley & Sons.
Parajo, J.C., Alonso, J.L., Vasquez, D., 1993. On the behavior of lignin and hemicellulose during acetosolv processing of wood. Bioresour. Technol. 46, 233–240.
Parschetti, G., Hoekman, S.K., Balasubramanian, R., 2013. Chemical, structural and combustion characteristics of carbonaceous products obtained by hydrothermal carbonization of palm empty fruit bunches. Bioresour. Technol. 135, 683–689.
Regmi, P., Moscoso, J.L., Kumar, S., Cao, X., Mao, J., Schafran, G., 2012. Removal of cupper and cadmium from the aqueous solution using switchgrass biochar produced via hydrothermal carbonization process. J. Environ. Manage. 109, 61–69.
Reza, M.T., Uddin, M.H., Lynam, J.G., Coronella, C.J., 2013a. Hydrothermal carbonization: fate of inorganics. Biomass Bioenergy 49, 86–94.

Reza, M.T., Uddin, M.H., Lynam, J.G., Hoekmann, S.K., Coronella, C.J., Vasquez, V.R., 2013b. Reaction kinetics and particle size effect on hydrothermal carbonization of loblolly pine. Bioresour. Technol. 139, 161–169.

Reza, M.T., Uddin, M.H., Lynam, J.G., Hoekmann, S.K., Coronella, C.J., 2014. Hydrothermal carbonization of loblolly pine: reaction chemistry and water balance. Biomass Conv. Bioref.. http://dx.doi.org/10.1007/s13399-014-0115-9.

Rillig, M.C., Wagner, M., Salem, M., Antunes, P.M., George, C., Ramke, H.G., et al., 2010. Material derived from hydrothermal carbonization: effects on plant growth and *Arbuscular mycorrhiza*. Appl. Soil Ecol. 45 (3), 238–242.

Sevilla, M., Fuertes, A.B., 2009. Chemical and structural properties of carbonaceous products obtained by hydrothermal carbonization of saccharides. Chem. Eur. J. 15, 4195–4203.

Szlyk, E., Szydlwska-Czerniak, A., Kowalczyk-Marzec, A., 2005. NIR spectroscopy and partial least-squares regression for determination of natural alpha-tocopherol in vegetable oils. J. Agric. Food Chem. 53, 6980–6987.

Titirici, M.M., Antonietti, M., 2010. Chemistry and materials options of sustainable carbon materials made by hydrothermal carbonization. Chem. Soc. Rev. 39, 103–116.

Uddin, M.H., Reza, M.T., Lynam, J.G., Coronella, C.J., 2013. Effects of water recycling in hydrothermal carbonization of loblolly pine. Env. Prog. Sus. Energy. http://dx.doi.org/10.1002/ep.11899.

UN Energy Report, 2007. Sustainable Bioenergy: A Framework for Decision Maker.

Weyer, L.G., 1985. Near-Infrared spectroscopy of organic substances. Appl. Spectrosc. Rev. 21 (1–2), 1–43.

Wiedner, K., Naisse, C., Rumpel, C., Pozzi, A., Wieczorek, P., Glaser, B., 2013. Chemical modification of biomass residues during hydrothermal carbonization – What makes the difference, temperature or feedstock? Org. Geochem. 54, 91–100.

Wirth, B., Mumme, J., 2013. Anaerobic digestion of waste water from hydrothermal carbonization of corn silage. Appl. Bioenergy 1, 1–10. http://dx.doi.org/10.2478/apbi-2013-0001.

Yang, M., Nie, S., Li, J., Xie, M., Xiong, H., Deng, Z., et al., 2010. Near-infrared spectroscopy and partial least-squares regression for determination of arachidonic acid in powdered oil. Lipids 45, 559–565.

Yu, L., Falco, C., Weber, J., White, R.J., Howe, J.Y., Titirici, M.M., 2012. Carbohydrate-derived hydrothermal carbons: a through characterization study. Langmuir 28, 12373–12383.